

## **REACTIVITY OF LITHIUM AND BARIUM CARBONATES WITH $ZrO_2:Y_2O_3$ AND NASICON IN SOLID STATE ELECTROCHEMICAL GAS SENSORS**

*P. Pasierb<sup>\*</sup>, R. Gajerski, S. Komornicki and M. Rękas*

AGH University of Science and Technology, Faculty of Materials Science and Ceramics,  
al. Mickiewicza 30, 30-059 Cracow, Poland

### **Abstract**

The mutual reactivity in mixtures containing Nasicon ( $Na_3Zr_2Si_2PO_{12}$ ) or YSZ ( $ZrO_2:Y_2O_3$ ) solid electrolytes with  $Li_2CO_3$  or  $Li_2CO_3:BaCO_3$  sensing electrode materials was investigated using simultaneous DTA and TG and ex situ XRD techniques. The uncontrolled chemical reaction is suspected to be responsible for the instability of electrochemical gas sensors constructed from these materials. DTA and TG results obtained for Nasicon-carbonate mixtures indicate the possibility of reaction in the temperature range from about 470 to 650°C, which overlaps the sensor operating temperature range (300–525°C). The results obtained for YSZ-carbonate mixtures indicate that reaction between carbonate and the  $ZrO_2$  takes place at higher temperatures and cannot explain the instability drift of investigated sensors. The mechanism of observed reactions in systems studied is also discussed.

**Keywords:** barium carbonate, DTA, electrochemical gas sensor, lithium carbonate, Nasicon, reactivity, TG, YSZ

### **Introduction**

There is a substantial interest in the development of  $CO_2$  gas sensors for application in food storage and packaging, environment monitoring or air conditioning systems. Such sensors should exhibit high selectivity and sensitivity, short response and recovery time, long-term signal stability, reproducibility and low cost of preparation. Among many proposed solutions, solid-state potentiometric gas sensors are considered to be the most promising, because of their high selectivity, simple structure and low cost of preparation. A typical potentiometric gas sensor consists of solid electrolyte (for example Nasicon,  $Na^+$   $\beta$ -alumina or  $ZrO_2$ ), sensing and reference electrodes attached from both sides of the solid electrolyte. In general, the measured electromotive force of such electrochemical cell is a function of partial pressure of  $CO_2$ , being in equilibrium with sensing electrode material. One of the important problems in the development of

\* Author for correspondence: E-mail: ppasierb@uci.agh.edu.pl

such sensing devices, leading to the future commercial application, is poor long-term stability of sensor signal.

According to thermodynamic calculations some undesired chemical reactions are suspected to be responsible for sensors instability during long-term operation. The purpose of this work was to investigate the possibility of chemical reaction between solid electrolyte and sensing electrode materials in the sensors working temperature range (300–525°C).

## Experimental

For our investigations Nasicon ( $\text{Na}_3\text{Zr}_2\text{Si}_2\text{PO}_{12}$ ) and YSZ ( $\text{ZrO}_2\text{:Y}_2\text{O}_3$  8 mol%) as a solid electrolyte materials and  $\text{Li}_2\text{CO}_3$  and  $\text{Li}_2\text{CO}_3\text{:BaCO}_3$  as sensing electrode materials were selected. These materials are commonly used in preparation of prototype  $\text{CO}_2$  sensors [1–10]. The  $\text{Na}_3\text{Zr}_2\text{Si}_2\text{PO}_{12}$  powder was prepared by coprecipitate method, as described elsewhere [11]. Obtained material was calcined at 1150°C and then wet milled (in absolute ethyl alcohol) in rotational-vibrational mill to an average grain size of 0.5  $\mu\text{m}$ . This material crystallised in monoclinic structure with usual slight admixture of  $\text{ZrO}_2$  phase, as derived from X-ray diffraction patterns. This is in agreement with the results reported elsewhere [11]. Commercially available powders of  $\text{ZrO}_2\text{:Y}_2\text{O}_3$  (Tosoh Corp., average grain size of 25 nm),  $\text{Li}_2\text{CO}_3$  (Aldrich, ReagentPlus<sup>TM</sup>, 99.99%) and  $\text{BaCO}_3$  (Aldrich, A.C.S. Reagent, 99%) were used as supplied. Before experiments the appropriate quantities of solid electrolyte and carbonate powders were mechanically dry mixed, the details concerning the composition of samples are given in Table 1.

**Table 1** Initial composition of prepared samples

No.	Solid electrolyte (SE)	Sensing electrode	SE: $\text{Li}_2\text{CO}_3$ : $\text{BaCO}_3$ (molar ratio)
1	YSZ ( $\text{ZrO}_2$ +8% $\text{Y}_2\text{O}_3$ )	$\text{BaCO}_3$	1:0:1
2	YSZ ( $\text{ZrO}_2$ +8% $\text{Y}_2\text{O}_3$ )	$\text{Li}_2\text{CO}_3$	1:1:0
3	YSZ ( $\text{ZrO}_2$ +8% $\text{Y}_2\text{O}_3$ )	$\text{Li}_2\text{CO}_3\text{:BaCO}_3$ (4:6)	5:2:3
4	Nasicon ( $\text{Na}_3\text{Zr}_2\text{Si}_2\text{PO}_{12}$ )	$\text{Li}_2\text{CO}_3\text{:BaCO}_3$ (4:6)	5:2:3

The mutual reactivity of these materials was investigated using differential thermal analysis (DTA) and thermogravimetry (TG) – (TA Instruments Derivatograph, type SDT 2960, equipped with the mass spectrometer Balzers Thermostar GSD 300 and DSC 2010 unit), scanning electron microscopy (SEM) – (JEOL JSM-5400) and X-ray diffraction (XRD) techniques – (Seifert XRD-7 Diffractometer with  $\text{CuK}_\alpha$  filtered radiation in the  $2\theta$  range from 10 to 60°, with step of 0.02° and sampling time 2 s).

## Results and discussion

Figure 1 shows the stability ranges of Li and Ba carbonates and corresponding zirconates calculated on the basis of thermodynamic data [12].

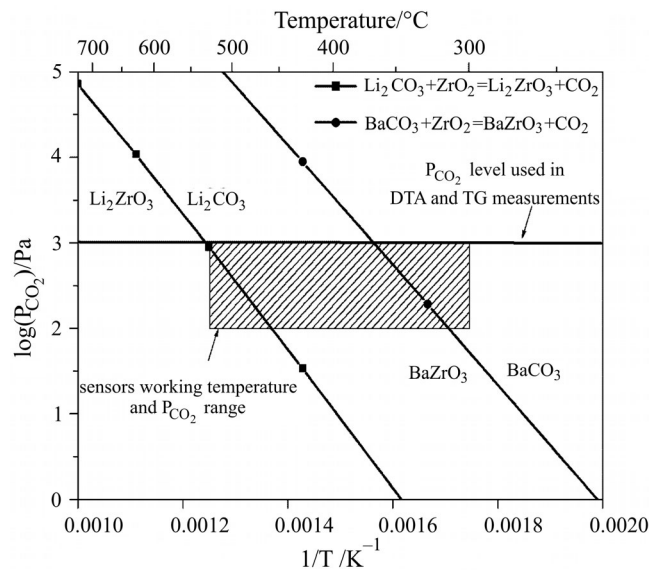


**Fig. 1** Stability ranges of  $\text{Li}_2\text{CO}_3$  and  $\text{BaCO}_3$  carbonates and corresponding zirconates  $\text{Li}_2\text{ZrO}_3$  and  $\text{BaZrO}_3$  calculated on the basis of thermodynamic data [12]. The hatched area covers the sensors working temperature and carbon dioxide partial pressure ranges, the horizontal line corresponds to the  $P_{\text{CO}_2}$  partial pressure used in DTA and TG measurements

The region above the lines corresponds to the stability region of the carbonates, the region below the lines corresponds to the stability region of corresponding zirconates. The hatched rectangle area covers the sensors operating range of carbon dioxide pressure and temperature, while the horizontal line corresponds to the carbon dioxide partial pressure used in DTA and TG measurements. On the basis of these calculations it can be stated that the reaction of carbonates and  $\text{ZrO}_2$  leading to the formation of zirconates (according to the reactions given in figure inset) is possible in this range of  $P_{\text{CO}_2}$  and  $T$ . It is not possible to propose a priori the mechanism of chemical reaction and perform the calculations in case of Nasicon-carbonate mixtures, because of complex composition of Nasicon and due to incomplete thermodynamic data.

In order to investigate the reactivity of solid electrolyte material ( $\text{Nasicon}$  or  $\text{ZrO}_2\cdot 8\% \text{Y}_2\text{O}_3$ ) with sensing electrode material ( $\text{Li}_2\text{CO}_3$ ,  $\text{BaCO}_3$  or  $\text{Li}_2\text{CO}_3\cdot\text{BaCO}_3$ ) different mixtures of powders were prepared by dry mixing of solid electrolyte material with carbonates (sensing electrode material). The composition of samples is given in Table 1.

Figures 2–5 show the results of DTA and TG measurements performed for samples 1–4, respectively. Measurements were done in the flow of artificial air containing 1.5 vol% of  $\text{CO}_2$ . The right axis corresponds to mass loss represented as the degree of complete decomposition of appropriate carbonates (abbreviated as  $\text{DCCD}$  [%]), calculated using the following formula:

$$DCCD[\%] = \frac{100 - TG[\%]}{W}$$

where  $TG[\%]$  is the determined percent mass residue of the sample, while  $W$  is the theoretical percent mass loss due to complete decomposition of carbonates in the mixture ( $W$  is equal to 13.38, 21.42, 15.74 and 6.49, for samples 1, 2, 3, and 4, respectively).

The results presented in Fig. 2 indicate clearly, that the reaction between barium carbonate and zirconium oxide does not take place in the temperature range covered ( $T=25-1000^{\circ}\text{C}$ ). This result does not comply with the thermodynamic calculations presented in Fig. 1, where the reaction is expected at temperatures lower than  $T=500^{\circ}\text{C}$  (even at relatively high carbon dioxide partial pressures), but may be explained by taking into account the kinetic aspects of the reaction and low diffusion coefficients of Ba or Zr in the material.

The endothermic peak observed at about  $815^{\circ}\text{C}$  (Fig. 2) corresponds to the  $\gamma$ - $\beta$  phase transition in  $\text{BaCO}_3$ . More details concerning the thermal properties of  $\text{Li}_2\text{CO}_3$  and  $\text{BaCO}_3$  carbonates can be found in [13, 14].

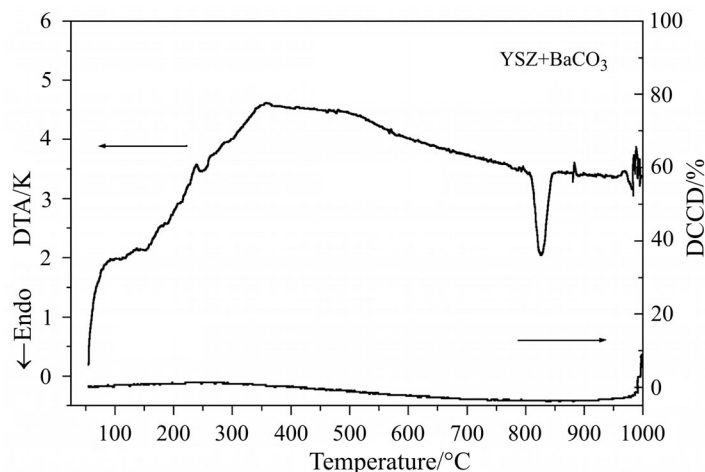
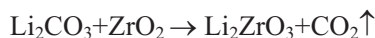


**Fig. 2** DTA and TG measurements performed for sample 1 ( $\text{YSZ}:\text{BaCO}_3$ ) in the flow of artificial air containing 1.5 vol% of  $\text{CO}_2$

The results presented in Fig. 3 indicate that in the case of sample 2 the chemical reaction starts at temperature about  $600^{\circ}\text{C}$ . The beginning of reaction can be observed as a rapid decrease of sample mass caused by  $\text{CO}_2$  liberation (shown as the increase of DCCD), according to the reaction:



According to literature data [13, 14] the decomposition of lithium carbonate (accompanied with  $\text{CO}_2$  liberation) starts at higher temperatures (above  $T=700^{\circ}\text{C}$ ). The endothermic peak observed on DTA curve may be attributed to the melting of lithium carbonate at  $T=727^{\circ}\text{C}$  [13, 14]).

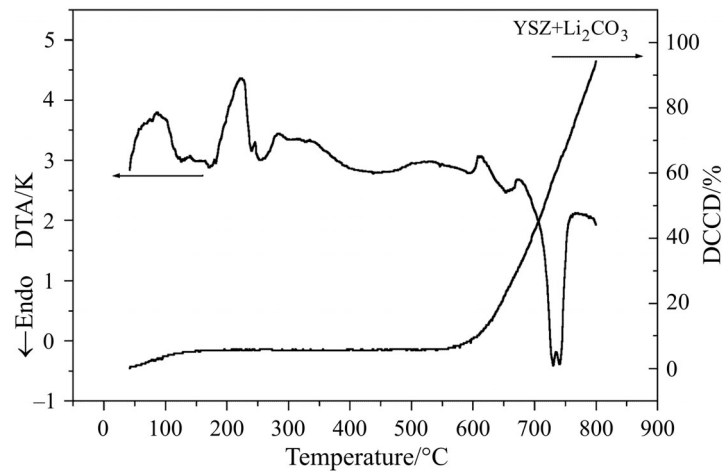


**Fig. 3** DTA and TG measurements performed for sample 2 (YSZ:Li<sub>2</sub>CO<sub>3</sub>) in the flow of artificial air containing 1.5 vol% of CO<sub>2</sub>

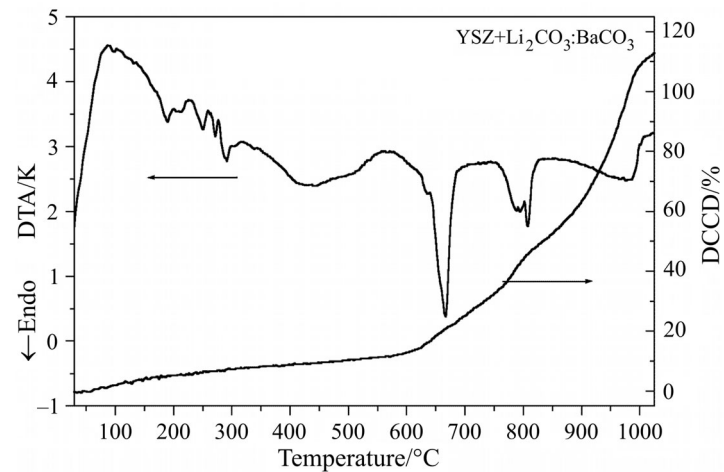


**Fig. 4** DTA and TG measurements performed for sample 3 (YSZ:Li<sub>2</sub>CO<sub>3</sub>:BaCO<sub>3</sub>) in the flow of artificial air containing 1.5 vol% of CO<sub>2</sub>

In case of sample 3 (ZrO<sub>2</sub>+Li<sub>2</sub>CO<sub>3</sub>:BaCO<sub>3</sub>, Fig. 4) a decrease of sample mass starts at temperature about 600°C, similarly as in the case of sample 2. The same temperature and similar composition suggest the formation of lithium zirconate as a primary product of reaction. The first endothermic peak observed on DTA curve in the temperature range  $T=630\text{--}690^\circ\text{C}$  may be attributed to the melting of lithium–barium carbonate mixture, according to the phase diagram of this eutectic system [14]. The second endothermic peak observed in the temperature range from 750–825°C can be partially interpreted in terms of  $\gamma$ – $\beta$  phase transition in BaCO<sub>3</sub> at 815°C [14] but its

complex shape, together with non-linear shape of TG curve suggest additional process or reaction taking place in this temperature range.

In the case of sample 4 ( $\text{Na}_3\text{Zr}_2\text{Si}_2\text{PO}_{12} + \text{Li}_2\text{CO}_3 : \text{BaCO}_3$ , Fig. 5) the reaction starts at about  $T=475^\circ\text{C}$ , where rapid mass loss can be noticed on TG curve. It is accompanied with complex endothermic peak (or two peaks) in the temperature range  $T=460\text{--}550^\circ\text{C}$ . The second endothermic peak observed in the temperature range  $T=600\text{--}680^\circ\text{C}$  may be attributed to the melting of lithium–barium carbonate mixture, as in the case of sample 3.

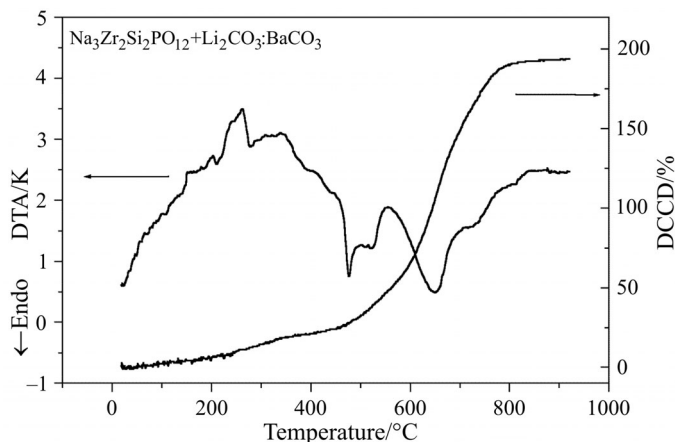


**Fig. 5** DTA and TG measurements performed for sample 4 ( $\text{Nasicon}:\text{Li}_2\text{CO}_3:\text{BaCO}_3$ ) in the flow of artificial air containing 1.5 vol% of  $\text{CO}_2$

As can be seen in Figs 3 and 4 the determined values of *DCCD* are higher than 100%. Thus the observed mass loss cannot be explained only by the decomposition of  $\text{Li}_2\text{CO}_3$  or  $\text{BaCO}_3$ . The evaporation of lithium at higher temperatures must be also taken into account.

The long-term operation of gas sensors takes place at elevated temperatures. In order to determine the limit of working temperature isothermal studies are necessary. Figure 6 shows the example results of isothermal TG measurements of samples 3 and 4, compared to the results obtained for  $\text{Li}_2\text{CO}_3:\text{BaCO}_3$  (2:3) and Nasicon materials. Upper graph of Fig. 6 shows the temperature profile during the measurement.

As can be seen in case of  $\text{Li}_2\text{CO}_3:\text{BaCO}_3$ ,  $\text{Na}_3\text{Zr}_2\text{Si}_2\text{PO}_{12}$  and  $\text{Li}_2\text{CO}_3:\text{BaCO}_3 + \text{ZrO}_2$  samples, no mass loss caused by the reaction can be noticed (Fig. 6). Slight decrease of mass at lower temperatures (especially in the case of Nasicon) can be explained in terms of water vapour desorption. However, in the case of  $\text{Li}_2\text{CO}_3:\text{BaCO}_3 + \text{Na}_3\text{Zr}_2\text{Si}_2\text{PO}_{12}$  sample the continuous decrease of sample mass can be noticed during the isothermal heating at  $T=525^\circ\text{C}$ . The measurement at  $T=425^\circ\text{C}$  shows the stable sample mass, thus indicating that there is no reaction at this temperature. These results are in agreement with the results presented in Fig. 5, where the start of reaction occurs at about  $T=475^\circ\text{C}$ .

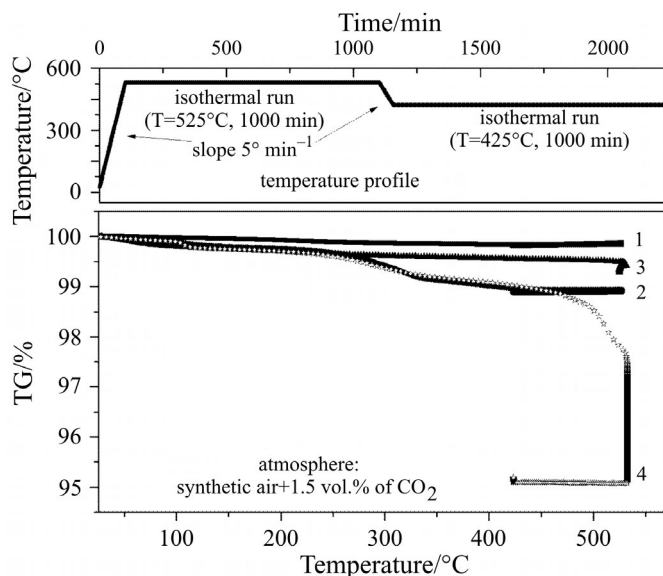


**Fig. 6** Isothermal TG measurement of 1 –  $\text{Li}_2\text{CO}_3:\text{BaCO}_3$ , 2 –  $\text{Na}_3\text{Zr}_2\text{Si}_2\text{PO}_{12}$ , 3 –  $\text{Li}_2\text{CO}_3:\text{BaCO}_3+\text{ZrO}_2$  and 4 –  $\text{Li}_2\text{CO}_3:\text{BaCO}_3+\text{Na}_3\text{Zr}_2\text{Si}_2\text{PO}_{12}$  samples, taken at 550 and 425°C. Upper graph shows the temperature profile during the measurement

In order to determine the phase composition of reaction products XRD measurements of heat-treated samples were performed. Figure 7 shows example results of XRD data obtained for sample 4 ( $\text{Na}_3\text{Zr}_2\text{Si}_2\text{PO}_{12}+\text{Li}_2\text{CO}_3:\text{BaCO}_3$ ) after heat treatment at  $T=800^\circ\text{C}$ , for 24 h. The heat treatment was done at higher temperature than DTA and TG measurements in order to allow complete reaction between Nasicon and carbonate.

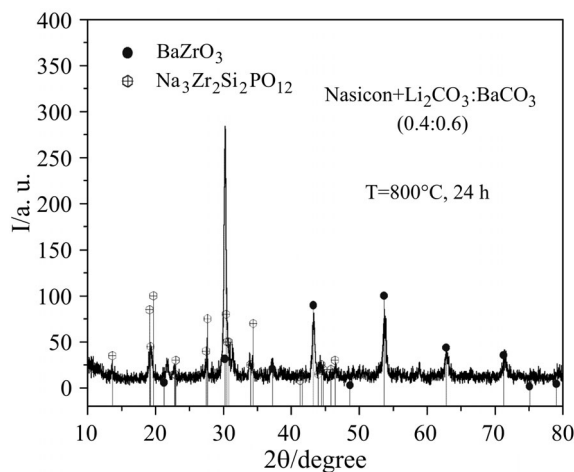


**Fig. 7** X-ray diffraction data obtained for sample 4 ( $\text{Na}_3\text{Zr}_2\text{Si}_2\text{PO}_{12}+\text{Li}_2\text{CO}_3:\text{BaCO}_3$ ), after heat treatment at  $T=800^\circ\text{C}$  for 24 h

The presented results allow to state that the dominant product of reaction is  $\text{BaZrO}_3$  cubic phase. Some reflexes of monoclinic Nasicon phase were also found.

In the case of heat-treated  $\text{ZrO}_2+\text{Li}_2\text{CO}_3$  and  $\text{ZrO}_2+\text{Li}_2\text{CO}_3:\text{BaCO}_3$  mixtures (samples 2 and 3) the obtained dominant products were  $\text{Li}_2\text{ZrO}_3$  and  $\text{BaZrO}_3$ , respectively.

Additional information concerning the mutual reactivity of solid electrolyte and sensing electrode materials can be also obtained from SEM observations. Figure 8 shows the example SEM image of sample 3 ( $\text{YSZ}+\text{Li}_2\text{CO}_3:\text{BaCO}_3$ ), after heat treatment at  $T=600^\circ\text{C}$  for 48 h. As can be seen, after heat treatment this multiphase system consists of round grains immersed in second phase. Also some island-like shapes can be observed in the middle of image, indicating the presence of liquid phase during the reaction.

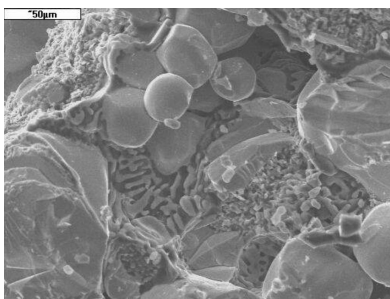


Fig. 8 SEM image of sample 3 ( $\text{YSZ}+\text{Li}_2\text{CO}_3:\text{BaCO}_3$ ) after heat treatment at  $T=600^\circ\text{C}$  for 48 h

## Conclusions

The DTA and TG results obtained for Nasicon –  $\text{Li}_2\text{CO}_3$  and  $\text{Li}_2\text{CO}_3:\text{BaCO}_3$  mixtures show several endo- and exothermal peaks, indicating complex reactions between carbonate and Nasicon. These peaks are observed in the temperature range from about  $470$  to  $650^\circ\text{C}$ , which covers the sensor operating temperature range.

The results obtained for  $\text{YSZ} - \text{Li}_2\text{CO}_3$  and  $\text{YSZ} - \text{Li}_2\text{CO}_3:\text{BaCO}_3$  mixtures indicate that the reaction between carbonate and the  $\text{ZrO}_2$  cannot explain the instability drift of investigated sensors. The observed decomposition of carbonates accompanied by the formation of appropriate zirconates takes place at higher temperatures than the working temperature of sensors.

\* \* \*

The financial support of Polish State Committee for Scientific Research (KBN), Project No. 7T08A03021 is acknowledged.

## References

- 1 N. Miura, Y. Yan, M. Sato, S. Nonaka and N. Yamazoe, *J. Mater. Chem.*, 5 (1995) 1391.
- 2 N. Yamazoe and N. Miura, *Solid State Ionics*, 86–88 (1996) 987.
- 3 M. Holzinger, J. Maier and W. Sitte, *Solid State Ionics*, 86–88 (1996) 1055.



- 4 M. Holzinger, J. Maier and W. Sitte, *Solid State Ionics*, 94 (1997) 217.
- 5 K. Nāfē, *J. Electrochem. Soc.*, 144 (1997) 915.
- 6 T. Kida, K. Shimano, N. Miura and N. Yamazoe, *Sens. Actuators*, B75 (2001) 179.
- 7 C. Favotto and P. Satre, *J. Therm. Anal. Cal.*, 68 (2002) 49.
- 8 N. Guillet, C. Pijolat and R. Lalauze, *J. Therm. Anal. Cal.*, 68 (2002) 15.
- 9 C. O. Park, C. Lee, S. A. Akbar and J. Hwang, *Sens. Actuators*, B88 (2003) 53.
- 10 P. Pasierb, S. Komornicki, R. Gajerski, S. Koziński and M. Rękas, *Solid State Ionics*, 157 (2003) 357.
- 11 J. P. Boilot, J. P. Salanie, G. Desplanches and D. Le Potier, *Mat. Res. Bull.*, 14 (1979) 1469.
- 12 O. Knacke, O. Kubaschewski and K. Hesselmann, Springer, Berlin 1991.
- 13 P. Pasierb, R. Gajerski, S. Komornicki and M. Rękas, *J. Therm. Anal. Cal.*, 65 (2001) 457.
- 14 P. Pasierb, R. Gajerski, M. Rokita and M. Rękas, *Physica B*, 304 (2001) 463.